

Effect of carbon black and nanoclay on mechanical and thermal properties of ABS-PANI/ABS-PPy blends

Narayan Debnath,¹ Vinay Panwar,² Souvik Bag,² Mitali Saha,¹ Kaushik Pal²

¹Department of Chemistry, National Institute of Technology Agartala, Tripura 247667, India

²Department of Mechanical and Industrial Engineering, Indian Institute of Technology Roorkee, Uttarakhand 247667, India

Correspondence to: K. Pal (E-mail: pl_kshk@yahoo.co.in)

ABSTRACT: Acrylonitrile butadiene styrene (ABS)–polyaniline (PANI) and ABS–polypyrrole (PPy) blends exhibit poor mechanical and thermal properties due to their weak interfacial adhesion and inhomogeneous mixing. The properties have been improved by addition of carbon black (CB) and nanoclay (NC). Composites are prepared by mixing CB and NC with ABS–PANI and ABS–PPy blends. The morphology and crystalline characteristics are studied using field emission scanning electron spectroscopy (FESEM) and X-ray diffraction, respectively. In addition, all the composites have been analyzed for their mechanical and thermal performance. The tensile strength of ABS–PANI has been increased by 7.18% and 65.83% with addition of CB and a combination of CB–NC, respectively. FESEM images are found supportive with these trends and show homogeneous dispersion of CB in the polymer matrix, assisted by NC. Dynamic mechanical analysis results also show slight improvement of glass transition temperature (T_g) with addition of fillers. © 2015 Wiley Periodicals, Inc. *J. Appl. Polym. Sci.* **2015**, *132*, 42577.

KEYWORDS: blends; clay; composites; conducting polymers; thermoplastics

Received 17 January 2015; accepted 4 June 2015

DOI: 10.1002/app.42577

INTRODUCTION

Thermoplastic-polymers-based nanocomposites are extensively used nowadays due to their suitability for variety of applications such as structural, energy storage, and sensors. Acrylonitrile butadiene styrene (ABS) is one of such thermoplastic polymer and is classified as a terpolymer composed of acrylonitrile, butadiene, and styrene.¹ It has been attracting attention of the researchers since 2000 mainly due to its good mechanical properties and ease of processability which makes it appropriate for general purpose engineering plastic.^{2–4} ABS exhibits good impact strength, temperature resistance against medium, excellent abrasion resistant, antistatic adjustment and can be machined into desired shaped products with good surface finish.⁵ In addition, it shows good resistance against UV light, aromatic hydrocarbons (i.e., benzene, benzoic acid), and organic solvents (i.e., isopropyl alcohol, diethyl ether). ABS itself is a nontoxic polymer but its combustion products are highly toxic.¹ Carbon-based nanofillers like carbon nanotubes (CNT) and carbon black (CB) have excellent electronic and mechanical properties which invite these fillers for their application in polymer composites by dispersing the fillers in polymer matrices.

Mechanical, rheological, and thermal properties of composites of ABS/CB have been studied by researchers since 2000.⁶ Ou *et al.*⁵ studied the electrical behavior of ABS–CB composites to

analyze the variation in percolation threshold for once and twice extruded composites. Shenavar *et al.*^{7,8} has shown the improvements in thermal stability, flow behavior, and mechanical properties (i.e., impact strength and Young's modulus) of ABS due to incorporation of CB in ABS matrix. Felix *et al.*⁹ performed similar study by incorporating sepiolite clay to ABS, with four different surfactant agents, resulting for increase in stiffness and decrease in toughness of ABS. Current research related to nanoclay (NC) and its polymer composites have proved that it offers enhanced thermal and mechanical properties with good processability and dispersibility. NC is a relatively cheap and readily available nanofiller. It has a high aspect ratio and a plate morphology which makes the material an efficient filler and reinforcing agent¹⁰. Montmorillonite is a class of magnesium aluminum silicate having sheet-like morphology, and can be used to make a new class of nanocomposites using polymer and nanoclay. The large surface area (750 m²/g) and high aspect ratio (70–150) of montmorillonite contribute to its advanced rheological characteristics.¹¹ A small amount of nanoclay (4%) may bring about a drastic change in mechanical properties of composites.^{4,12–15} It exhibits excellent flame retardant property and remarkably nontoxicity that makes it suitable for food packaging material and high-temperature-resistant materials.^{4,16–19}

Intrinsically conducting polymers (ICPs) such as polyaniline (PANI), polypyrrole (PPy), polythiophene (PTh), and their derivatives have been prepared and examined, for their blends with amorphous polymers, as a result of their enormous application potential in such cases. These conducting polymers have been studied with great attention in the last few decades due to their easy processability, good electrical properties, high specific capacity, cheap and easy preparation, and light weight. PPy and PANI are particularly attractive due to their relatively high conductivity, low cost, and ease of synthesis.²⁰ They are well capable to conduct electricity through them due to extended conjugation in the carbon-carbon backbone of the polymer molecule and thus replacing the conventional conducting fillers due to their improved processability for preparing conducting polymer composites having good mechanical properties and stability. These advances extended the practical applications of these composites for sensors,²¹ anticorrosive materials,²² heating elements,^{23,24} etc. Some major problems in blending of ICPs are associated with aromatic structure, interchain hydrogen bonds, and effective charge delocalization.²⁵

The poor mechanical stability of conducting polymers requires blending or copolymerization of these conducting polymers with amorphous polymers which can withstand for high temperatures, according to required processing conditions.^{26,27} In this article, the effects of CB and CB-NC have been investigated in the ABS-PANI and ABS-PPy blends. The changes in thermal and mechanical properties of composites have been studied for a better product specific utilization. Variation in internal and surface properties has been observed through FTIR, XRD, and FESEM.

EXPERIMENTAL

Materials

Carbon black (P842) was obtained from Philips Carbon Black Ltd. Nanoclay (Cloisite-25a) was purchased from Connell Brothers, California, USA. CB and NC were dried in vacuum at 80°C for 48 h before used as filler. ABS was purchased (color: yellowish white, density: 1.045 g/cc, melt flow: 43 g/10 min @ 10.0 kg) from Bhansali Engineering and used as received without any further treatment. PANI and PPy were prepared as follows.

Preparation of Polyaniline. PANI was prepared according to the method given by Stejskal *et al.*²⁸ Aniline hydrochloride (0.2 M) was prepared by dissolving 2.59 g of aniline hydrochloride with double distilled water in a volumetric flask up to 50 mL. Ammonium peroxodisulphate (0.25 M) was prepared by dissolving 5.71 g of ammonium peroxodisulphate with double distilled water in a 50 mL volumetric flask. The solutions were kept at room temperature for 1 h. Both the solutions were mixed slowly with mild stirring and kept for polymerization with continuous stirring. After 8 h, the precipitates of PANI were collected by filtering. Washed with three 100 mL portion of 0.2 M HCl solution and similarly with acetone. PANI was dried in vacuum at 60°C for 24 h, grinded and again dried till a constant weight was achieved.

Preparation of Polypyrrole. PPy was prepared according to the Saravanan *et al.*²⁹ Paratoluene sulphonic acid (p-TSA) (3.84 g) was dissolved in 20 mL of double distilled (DD) water in round-bottom flask. Again 0.67 g pyrrole monomer (purified by distillation before reaction) was dissolved in 30 mL of double distilled water. Pyrrole solution was added in round-bottom flask containing p-TSA solution under stirring. Sodium lauryl sulphate (SLS) solution (1 g SLS dissolved in 20 mL of DD water) was further added to the solution. Benzoyl peroxide (BPO) (2.9 g) dissolved in 30 mL chloroform was then drop wise added in the mixer and the solution was kept for 3 h at room temperature. Reaction mixture was poured in acetone for precipitation. Black precipitate collected by filtration was washed with acetone and dried at 100°C in an oven until a constant weight was achieved.

Composite Preparation. Composites were prepared using internal mixer and compression molding machines. Their composition has been shown in Table I. For composite preparation, CB, NC, PANI, and PPy were dried at 80°C in oven before mixing. The base polymer (ABS) was allowed to heat inside the internal mixer at 220°C rotating at 60 rpm. When the matrix turns into a semisolid mass, fillers were added to the internal mixer through a hooper and allowed to mix up homogeneously. The composites were then placed in the cavities of a mould and molded in compression molding under 3 tons of pressure at 150°C for around 5 min. All the samples were allowed to cool down to room temperature slowly and then collected for different characterizations.

Characterizations

Morphology and Crystallinity. Fourier transform infrared (FTIR) spectroscopy of CB has been done using FTIR Spectrometer (Thermo Scientific, Nicolet 6700) to determine the functional groups present over the surface of the CB.

Field emission scanning electron microscopy (FESEM) has been done to study the surface morphology using FESEM Zeiss-Ultra Plus, Gemini Co., under a pressure of 1026 mBar. Fractured ends of the specimens left after tensile test were mounted on aluminum stubs, and a secondary electron (SE) detector was used to analyze the electrons. The gold coating on the abraded surface was used to make the surface conductive for the morphological analysis.

X-ray diffraction (XRD) plots were obtained with an X-ray diffractometer (Bruker AXS Diffraktometer D8) having Cu K α radiation ($\lambda = 0.154$ nm). All the scans were taken with a scan rate of 2°/min in the range of $2\theta = 10-90^\circ$. The current and operating voltage were maintained at 20 mA and 40 kV, respectively.

Mechanical Properties. Tensile test was carried out with a universal tensile testing machine (Instron 5582), at room temperature $25 \pm 2^\circ\text{C}$. Specimens for tensile testing were prepared according to ASTM D638-10. The initial gauge length of the specimens was 50 ± 5 mm, and the cross-head speed was maintained at 2 mm/min. Tensile strength (MPa), elongation at break (%), and ductility (%) were recorded from the stress-strain curve.

Dynamic mechanical analysis (DMA) was conducted using DMA machine (TA-Q800, USA). Loss modulus, storage modulus, and

Table I. Composition and Mechanical Properties of Different Composites

Sample codes	Elements (wt %)					Glass transition temp. (°C)	Tensile strength (MPa)	Elongation (%)
	ABS	PANI	PPY	CB	NC			
S1	100	-	-	3	-	109.8	19.7	3.5
S2	100	3	-	-	-	110.0	11.5	2.0
S3	100	3	-	3	-	111.5	12.5	1.6
S4	100	3	-	3	3	111.0	19.2	1.9
S5	100	-	3	-	-	110.3	22.0	2.2
S6	100	-	3	3	-	110.8	19.5	1.8
S7	100	-	3	3	3	111.7	25.0	1.4

tan delta were plotted with varying temperature (35–120°C) under 5°C/min ramp. The process of sample preparation for DMA was the same as for tensile testing. However, the specimen obtained from after hot press treatment were of rectangular shape having a dimension of 60 × 12 × 2 mm, as per design requirement of 3-point bending DMA clamp.

Thermal Properties. The thermal characteristics of all the nanocomposites were studied through TGA (TGA-SII 6300 Exstar Instrument). Thermal decomposition behavior of the nanocomposites was analyzed under increasing temperature. All the tests were carried out in nitrogen atmosphere at a scanning rate of 10°C/min and temperature range of 32–700°C. The initial weight of the all the samples was around 10–11 mg each.

To assess the phase change and the corresponding enthalpy change during the transition, DSC was performed using Perkin Elmer DSC-4000. All these tests were also performed under nitrogen atmosphere at a scanning rate of 10°C/min and a temperature range of 50–160°C.

RESULTS AND DISCUSSION

FTIR spectroscopy was carried out to ascertain the presence of functional groups on the surface of the CB and shown in Figure 1. A broad peak at 3435 cm⁻¹ indicates the presence of O—H

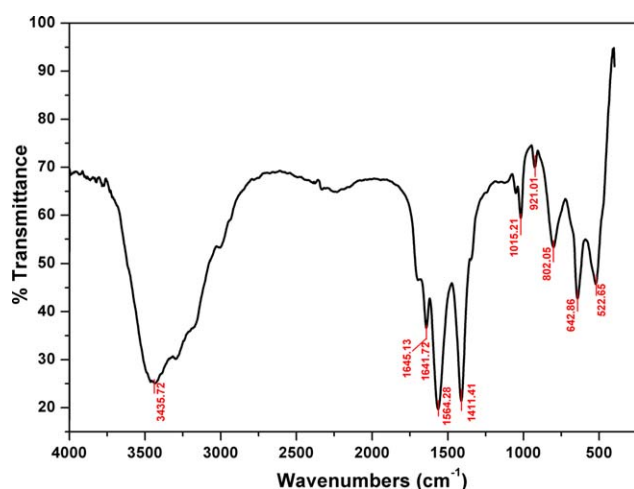


Figure 1. FTIR spectrum of CB (P842). [Color figure can be viewed in the online issue, which is available at wileyonlinelibrary.com.]

group and can be attributed to hydrogen-bonded phenolic or alcoholic O—H group.³⁰ The peak at 1645 cm⁻¹ is due to the presence of C=C. There is a probability of the presence of aromatic C—H (C=C—H), whose bending vibration is confirmed by a sharp peak at 1411 cm⁻¹ but its stretching vibration peak may be overlapped with the O—H stretching peak. Peak around 1015 cm⁻¹ is evident to the presence of =C—O stretching. At the lower frequencies, C—H bending vibrations are also observed. A sharp peak at 1641 cm⁻¹ indicates the presence of C=C stretching and two other sharp peaks at 1564 and 1411 cm⁻¹ indicates C—C stretching which is attached to sp²-hybridized C atom (i.e., C=C). All the three peaks altogether confirm the graphitic nature of the CB surface.

XRD analysis has been done for all the composite samples to determine their crystalline nature and filler–matrix intermixing. Corresponding results are shown in Figure 2. Carbon-based materials such as CB, carbon nanotube, carbon quantum dot, etc. shows XRD peak at 2θ = 25° for d₀₀₂.^{31–33} Virgin ABS also shows XRD peak at 20°. One characteristic peak is found to be common in all the samples at the range of 2θ = 20°–23° which is indicative of interlayer distance (d-spacing) increment and consequently good intermixing of filler and matrix.³⁴ Peak at 20° for S2 and S5 have become sharp comparing to pure ABS.

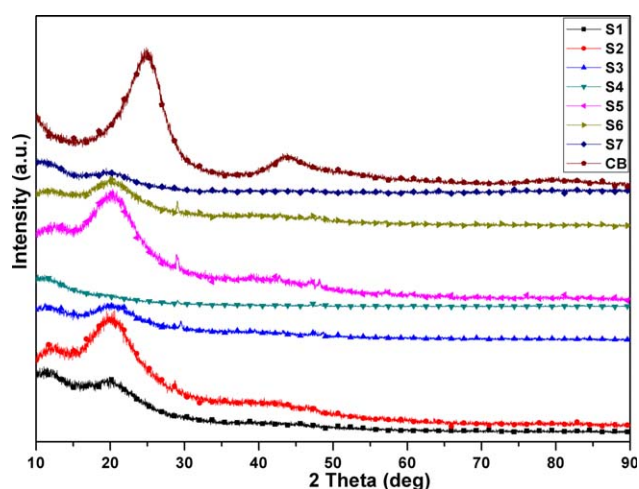


Figure 2. XRD spectra of different composites. [Color figure can be viewed in the online issue, which is available at wileyonlinelibrary.com.]

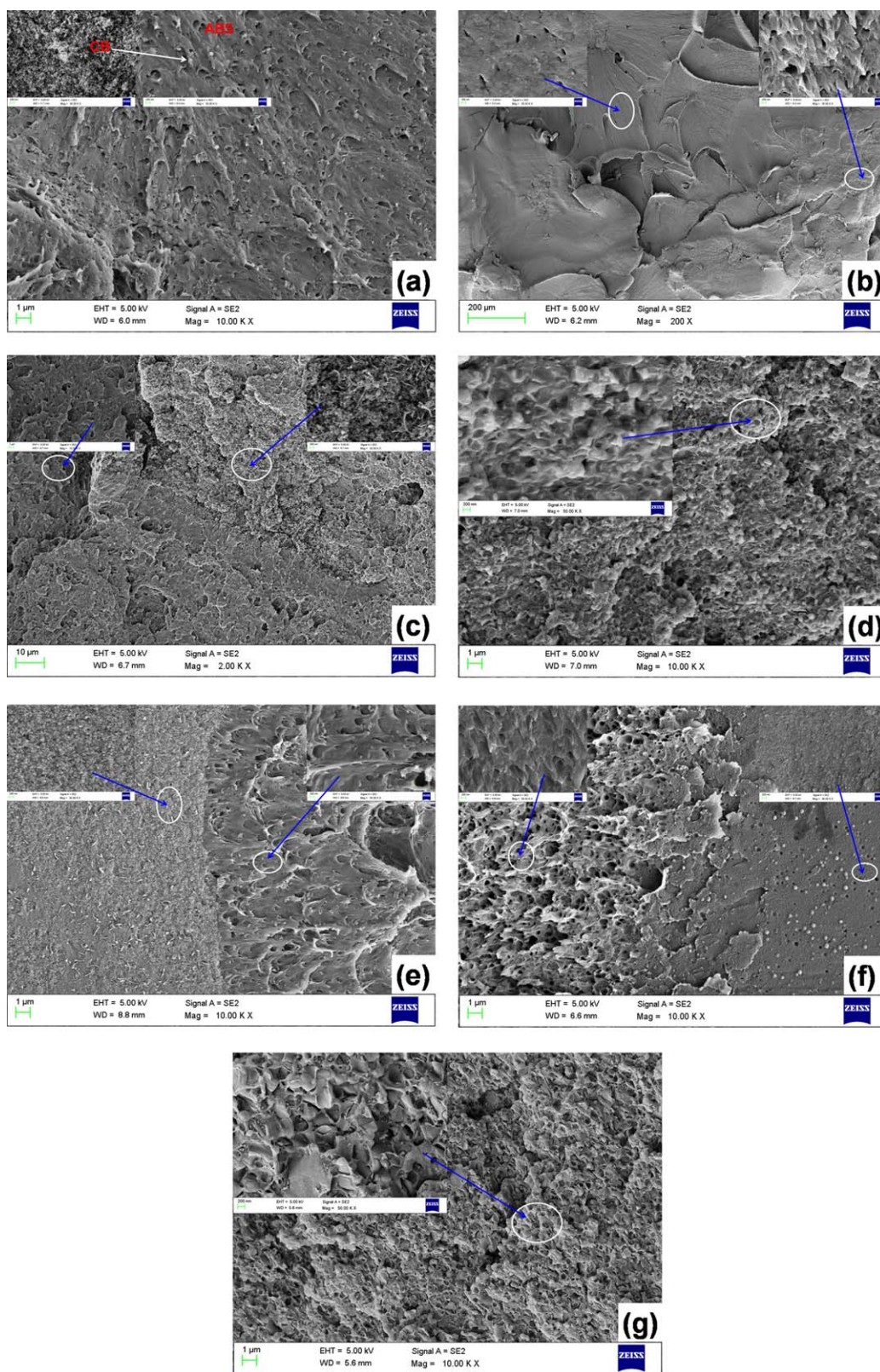


Figure 3. FESEM images of (a) CB and S1; (b) S2; (c) S3; (d) S4; (e) S5; (f) S6; (g) S7. [Color figure can be viewed in the online issue, which is available at wileyonlinelibrary.com.]

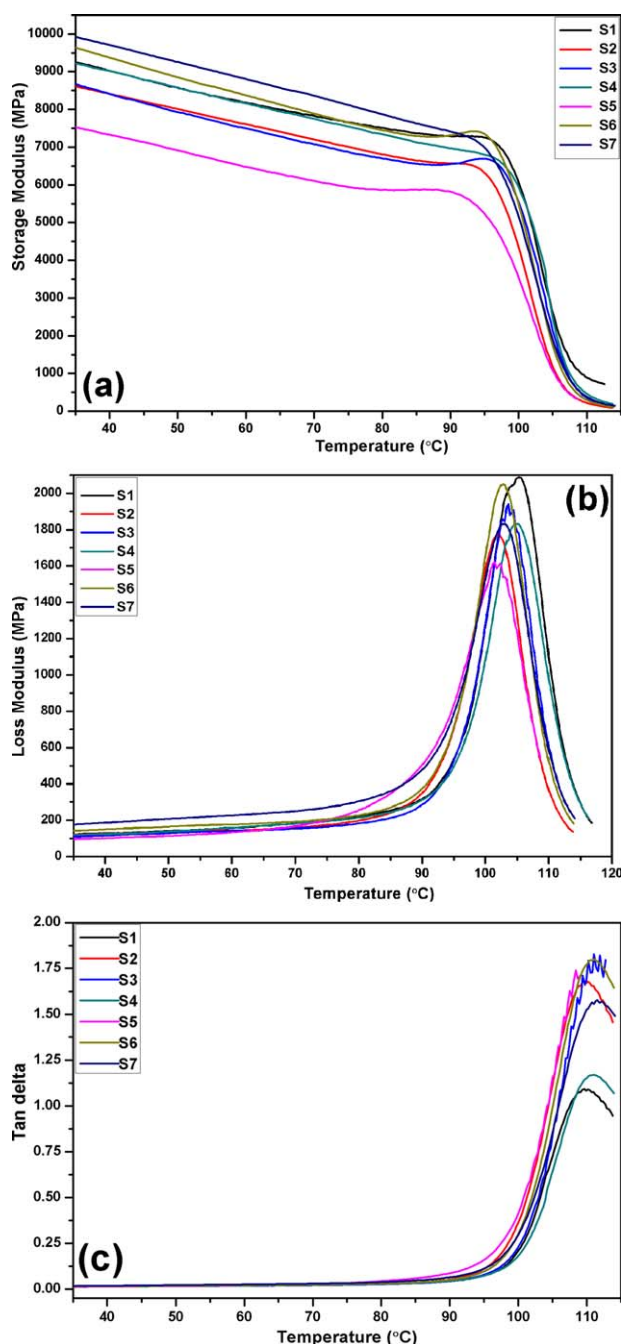


Figure 4. DMA of composites: (a) storage modulus vs temperature; (b) loss modulus vs temperature; (c) $\tan \delta$ vs temperature. [Color figure can be viewed in the online issue, which is available at wileyonlinelibrary.com.]

The mixing and interfacial adhesion of ABS/PANI and ABS/PPy blends shows crystallinity in nature. With addition of CB, the peak intensity decreased and peak area broadened in S3 and S6. This shows that the crystalline nature of ABS–PANI/PPy is decreased and amorphous characteristics are developed in the matrix due to incorporation of CB. This result is identical with that of S1 which clearly indicates that there is no effect of PANI and PPy on the crystal characteristics of ABS in the mentioned blends. Also, S4 and S7 composites are completely amorphous

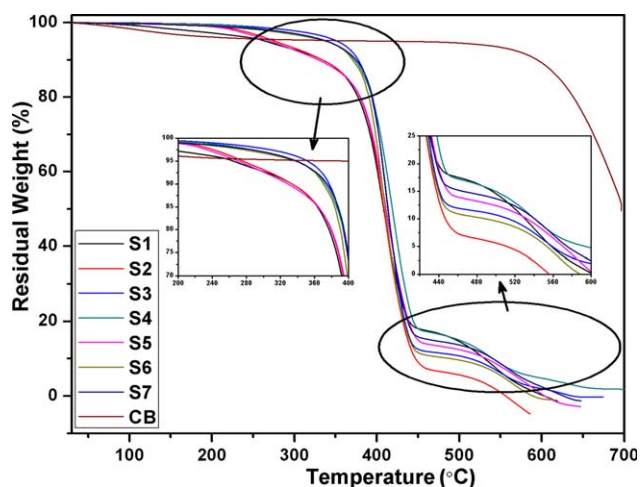


Figure 5. TGA thermograph of composites. [Color figure can be viewed in the online issue, which is available at wileyonlinelibrary.com.]

due to better dispersion of CB, assisted by NC, in the interstitial sites of the polymer matrix. NC here plays a crucial role in well mixing and interfacial adhesion of polymer and CB. This is further investigated and confirmed by FESEM.

FESEM has been done to observe the interfacial adhesion and dispersion of fillers in the polymer matrix using fractured end of samples obtained after tensile test. FESEM images of different composites used in this work have been shown in Figure 3. Figure 3(a) shows good dispersion of filler and polymer in ABS/CB composite. XRD peak of ABS/CB composite also supports this information. Figure 3(b and e) indicates poor mixing and weak interfacial adhesion of the two polymer components in ABS/PANI and ABS/PPy blends, respectively. This is in good agreement with the poor mechanical properties of composites. The presence of CB in polymer blend can be clearly observed in Figure 3(c and f), however, the dispersion seems to be highly nonuniform. NC plays an important role in the dispersion of filler in polymer matrix.³⁵ It may enter into the interstitial sites of the ABS matrix which allows the small CB particle to

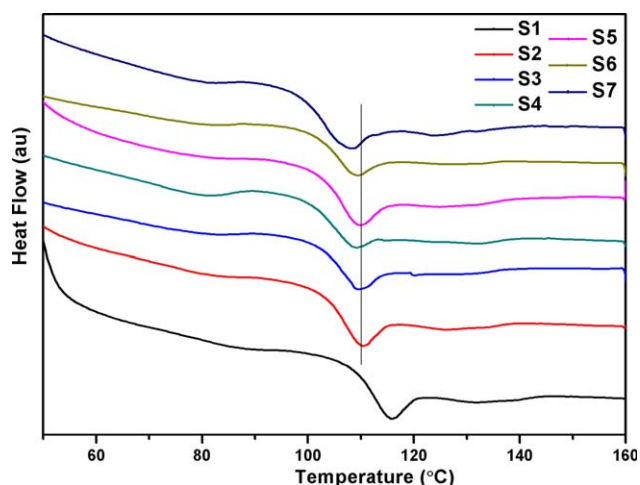


Figure 6. DSC thermograph of different composites. [Color figure can be viewed in the online issue, which is available at wileyonlinelibrary.com.]

Table II. Glass Transition Temperature and Enthalpy Change (ΔH) Through DSC Curves

Sample code	T_g ($^{\circ}\text{C}$)	ΔH (J/g)
S1	116.0	2.21
S2	110.5	0.74
S3	109.7	0.83
S4	109.0	1.53
S5	110.0	0.90
S6	109.1	1.63
S7	107.7	2.02

penetrate through the intermolecular layers of the matrix. The effect can clearly be observed in Figure 3(d and g), where NC assisted for improved mixing of the polymers (ABS–PANI and ABS–PPy), preparing blends, and better dispersion of CB in the blends.

Dynamic mechanical analysis (DMA) is employed to investigate the response of a material when a sinusoidal force is applied on it. This provides information regarding variation in storage modulus, loss modulus, and tan delta of specimen with varying temperature. Reinforcement of fillers in polymer nanocomposites enhances storage modulus. As the result of better reinforcing effect, the storage modulus must improve. The improvement of storage moduli of the nanocomposites is also due to the restricted chain mobility of chain segments of ABS due to the dispersion of CB and NC. Tan delta or damping factor is a measure of the impact resistance of a material. And it is associated with the movement of small groups and chains segments of polymer molecules within the polymer matrix. There is a possibility of mobility of phenyl and cyano groups present in ABS matrix due to the incorporation of fillers which leads to better damping of the prepared nanocomposites. In a composite system, damping is affected through the incorporation of fillers which is mainly due to shear stress relaxation through the additional viscoelastic energy dissipation in the matrix.

The DMA data has been shown in Figure 4. In Figure 4(c), the peak point in tan delta vs temperature curve is taken as glass transition temperature (T_g). Since after this temperature polymer turns into more elastic form, from a rigid state.^{36,37} The T_g values are compared in Table I. All the samples show high-temperature transition (α -transition). Composites S2 and S5 shows low storage modulus, loss modulus values. The corresponding values have been increased with addition of CB as can be observed through S3 and S6 curves. In Figures 4(a and b), with addition of NC, storage modulus has been noticed to increase whereas loss modulus decreases which finally result in high reduction of its internal damping. This can be clearly observed through S4 and S7 curves of Figure 4(c).

Tensile properties of composites are compared summarized in Table I, which shows the improvement of mechanical properties of ABS–PANI and ABS–PPY blends due to addition on filler. ABS–PANI blend is ductile and its elastic limit is very less compared to other samples. On addition of CB, its rigidity increases slightly. Whereas, NC-assisted dispersion of CB makes it more

brittle, rigid, and tough. Similar trend is noticed in case of ABS–PPY blend where S7 shows excellent rigidity, toughness, and brittleness. One noticeable fact is that the mixing of NC along with CB in both the blends increases the brittleness as well as the rigidity and toughness to a greater extent. This may be due to the well dispersion of CB in the polymer matrix assisted by the NC as observed from FESEM images.

In Figure 5, the residual weight due to heating is plotted against temperature. TGA curve for CB shows high thermal stability, up to 600 $^{\circ}\text{C}$ there is insignificant change in weight. A sudden dip around 600 $^{\circ}\text{C}$ indicates the degradation of CB. However, even up to 700 $^{\circ}\text{C}$, the residue remains 50%. S1, S2, and S5 show degradation from 200 to 360 $^{\circ}\text{C}$. This small decomposition resembles with that of the pure ABS indicating the poor mixing of ABS with PPy and PANI. Poor processability is one of the disadvantages of conducting polymers like PPy and PANI due to their rigid backbone.³⁸ Generally, they are not well mixed in thermoplastic polymers. Therefore, the mechanical and thermal properties of the blends resemble that of pristine ABS. The objective of this work is to develop these properties by the mixing and consequent reinforcement of fillers like CB and NC. CB and NC in those composites act as heat absorber and fillers and do not allow the heat build up by dissipating more heat than the polymer matrix. ABS–PANI or ABS–PPy blends, having better thermal stability (up to $\sim 230^{\circ}\text{C}$) over virgin ABS, improves the stability to $\sim 350^{\circ}\text{C}$. In fact, the addition of NC has no significant effect on thermal properties of these composites but as proved through XRD and FESEM, they support for uniform dispersion of CB.

The DSC results shown in Figure 6 are well supporting the DMA observations. T_g values and corresponding enthalpy change (ΔH) are shown in Table II. The positive value of ΔH for all the composites indicates endothermic phase change. ABS–PANI and ABS–PPy blends show very less ΔH value than reinforced samples. ΔH values have been increased for S3 and S6, this may be possibly due to establishment of CB–matrix interaction. Improvement in interaction could be due to the covalent bonding between functional groups present in CB and polymer, or weak van der Waals force among CB and matrix. Thus more energy will be consumed during the phase transition of the composites. In S4 and S7, NC also participates to enhance the interfacial interaction between polymers and dispersion of CB in blend. Consequently, ΔH values of composites increased by large extent.

CONCLUSIONS

In this work, we have studied the morphological, mechanical, and thermal properties of composites, prepared by mixing of CB to ABS–PANI/ABS–PPY blends, with and without NC. FESEM images show good dispersion of CB in the polymer matrix in the presence of NC which resulted for the improvement in mechanical properties of CB–NC-reinforced composites. Similar trend is observed from XRD analysis where the change of crystalline behavior of composites also confirms the better dispersion of CB in presence of NC. Enhancement of mechanical properties essentially is due to improved dispersion

and good interfacial adhesion among CB and the matrix. The development of polymer–filler covalent bonding or weak interactions through the functional groups of CB and NC may also be a reason for the change in mechanical properties. The trend for T_g through DMA and DSC are almost similar. Higher values of enthalpy change indicate the development of filler–matrix interaction probably through weak van der Waals interaction. Moreover, TGA notify that the high-temperature thermal stability of polymer blends has been introduced by CB.

REFERENCES

- Joseph, V. R.; Barbara, C. L. *Fire Mater.* **1986**, *10*, 93.
- Lu, M. L.; Lee, C. B.; Chang, F. C. *Polym. Eng. Sci.* **1995**, *35*, 1433.
- Alekseev, A. A.; Abdulrahim, R. M.; Osipchik, V. S.; Kirichenko, E. A.; Chernyshova, V. N. *Int. Polym. Sci. Technol.* **2003**, *30*, T18.
- Mohamed, H. G.; Nguyen, T. P.; Mohammad, A. A.; Kazuya, O.; Kiyoshi, U.; Isao, K.; Toru, F. *Cellulose* **2013**, *20*, 819.
- Ou, R.; Gerhardt, R. A.; Marrett, C.; Moulart, A.; Colton, J. S. *Compos. Part B* **2003**, *34*, 607.
- Yihu, S.; Chunfeng, X.; Qiang, Z. *Soft Matter* **2014**, *10*, 2685.
- Shenavar, A.; Abbasi, F.; Razavi, M. K.; Aghjeh, A. Z. *J. Thermoplast. Compos. Mater.* **2009**, *22*, 753.
- Shenavar, A.; Abbasi, F. *J. Appl. Polym. Sci.* **2007**, *105*, 2236.
- Felix, C. B.; David, G.; Norky, V.; Juan, C. M.; Jose, M. P. *Compos. Part B* **2012**, *43*, 2222.
- Tjong, S. C.; Jiang, W. J. *J. Appl. Polym. Sci.* **1999**, *73*, 2985.
- Man-Wai, H.; Chun-Ki, L.; Kin-tak, L.; Dickon, H. L. N.; David, H. *Compos. Struct.* **2006**, *75*, 415.
- Kojima, Y.; Usuki, A.; Kawasumi, M.; Okada, A.; Fukushima, Y.; Kurauchi, T. *J. Mater. Res.* **1993**, *8*, 1185.
- McNally, T.; Raymond, M. W.; Lew, C. Y.; Turner, R.; J.; Brennan, G. P. *Polymer* **2003**, *44*, 2761.
- LeBaron, P. C.; Wang, Z.; Pinnavaia, T. J. *Appl. Clay Sci.* **1999**, *15*, 11.
- Alexandre, M.; Dubois, P. *Mater. Sci. Eng.* **2000**, *28*, 1.
- Gilman, J. W. *Appl. Clay Sci.* **1999**, *15*, 31.
- Suqing, C.; Baishen, S.; Guobo, H.; Haichang, G.; Shuqu, W. *J. Vinyl Add. Tech.* **2013**, *19*, 285.
- Bin, L.; Zhaoshun, Z.; Hongfeng, Z.; Caiying, S. *J. Vinyl Add. Tech.* **2014**, *20*, 10.
- Maryam, A.; Seyed, M.; Zebarjad, E.; Goharshadi, K. *J. Vinyl Add. Tech.* **2014**, DOI: 10.1002/vnl.21443.
- Bora, C.; Dolui, S. K. *Polym. Int.* **2013**, *63*, 1439.
- Gangopadhyay, R.; De, A. *Sens. Actuator B* **2001**, *77*, 326.
- Wessling, B.; Posdorfer, J. *Electrochim. Acta* **1999**, *44*, 2139.
- Jonas, F.; Heywang, G. *Electrochim. Acta* **1994**, *39*, 1345.
- Stenger-Smith, J. D. *Prog. Polym. Sci.* **1998**, *23*, 57.
- Vikki, T.; Pietila, L. O.; Sterholm, H.; Ahjopalo, L.; Takala, A.; Toivo, A. *Macromolecules* **1996**, *29*, 2945.
- Shacklette, L. W.; Han, C. C. *Synth. Met.* **1993**, *55*, 3532.
- Avlyanov, J. K. *Synth. Met.* **1999**, *102*, 1272.
- Stejskal, J.; Gilbert, R. G. *Pure Appl. Chem.* **2002**, *74*, 857.
- Saravanan, C.; Shekhar, R. C.; Palaniappan, S. *Macromol. Chem. Phys.* **2006**, *207*, 342.
- Malas, A.; Das, C. K.; Das, A.; Heinrich, G. *Mater. Des.* **2012**, 39410.
- Athreya, S. R.; Kalaitzidou, K.; Das, S. *Compos. Sci. Technol.* **2011**, *71*, 506.
- Puvvada, N.; Prashanth, B. N. K.; Konar, S.; Kalita, H.; Mandal, M.; Pathak, A. *Sci. Technol. Adv. Mater.* **2012**, *13*, 7.
- Bao-Ku, Z.; Shu-Hui, X.; Zhi-Kang, X.; You-Yi, X. *Compos. Sci. Technol.* **2006**, *66*, 548.
- Malas, A.; Pal, P.; Giri, S.; Mandal, A.; Das, C. K. *Compos. Part B* **2014**, *58*, 267.
- Sharma, P.; Panwar, V.; Pal, K. *J. Appl. Polym. Sci.* **2015**, *132*, DOI: 10.1002/app.41477.
- Ehsani, M.; Borsi, H.; Gockenbach, E.; Morshedian, J.; Bakhshandeh, G. R. *Eur. Polym. J.* **2004**, *40*, 2495.
- Rieger, J. *Polym. Test.* **2001**, *20*, 199.
- Zhang, Y.; Rutledge, C. G. *Macromolecules* **2012**, *45*, 4238.